American Mineralogist, Volume 88, pages 748–762, 2003

Expandability of anchizonal illite and chlorite: Significance for crystallinity development in the transition from diagenesis to metamorphism

SALAH SHATA,[1,†] REINHARD HESSE,[1] ROBERT F. MARTIN,[1] AND HOJATOLLAH VALI[2,*]

[1]Department of Earth and Planetary Sciences, McGill University, Montreal, Québec, H3A 2A7, Canada
[2]Electron Microscopy Centre, McGill University, Montreal, Québec, H3A 2B2, Canada

ABSTRACT

In mixed-layer illite/smectite containing >80% illite, the presence of an expandable component and changes in its abundance are difficult or impossible to detect with the X-ray diffraction (XRD) method using conventional polar interstratification compounds, e.g., solvation with ethylene glycol. Although high-grade diagenetic and very low-grade metamorphic (VLGM) samples do not expand in response to ethylene glycol treatment, the illite crystallinity (IC) improves significantly with increasing diagenetic/metamorphic grade. Improvement of IC in anchizonal to epizonal samples previously was thought to be related primarily to increase in crystallite thickness and decrease in the number of stacking faults. The present study reexamines the contribution of expandable components to IC in shale and slate samples from the Gaspé Peninsula for both the <2 μm and <0.1 μm size fractions in the high-grade diagenetic and VLGM zone. As tools, we have used XRD patterns and high-resolution transmission electron microscopy (HRTEM) lattice-fringe images of samples treated with *n*-alkylammonium cations. These studies reveal the presence of expandable components including R1- and R3-ordered structures and "expandable illite." Expandable 2:1 clay minerals decrease in abundance with increasing metamorphic grade. The improvement of IC with grade is due to the decrease in expandable layers and also to the decrease in the number of lattice defects and an increase in crystallite size. Stacking faults may be the main source of lattice distortion only when phyllosilicates consist of thick non-expandable layer silicates.

During late diagenesis, the chlorites become ordered and are stabilized. They are the dominant phyllosilicate minerals present together with illites in the illite-chlorite facies of the anchizone. Lattice fringe images and XRD patterns document the presence of a short-range, corrensite-like R1 ordered phase and thick chlorite packets.

INTRODUCTION

Illite crystallinity, measured as full-width at half-maximum (FWHM) of the 10 Å X-ray diffraction (XRD) peak of illitic materials, is an empirical index used to characterize the grade of diagenesis or very low-grade metamorphism (VLGM) in terranes where index minerals and diagnostic mineralogical assemblages are not available. Because of the simplicity of measurements of illite crystallinity (hereafter, IC), this property has been widely used over the last 40 years, generally in conjunction with other parameters of maturity such as organic-matter reflectance, to establish diagenetic and very low-grade metamorphic (VLGM) conditions. Yet, interpretations of the physical meaning of the FWHM of the 10 Å reflection of illite in anchizonal and higher-grade rocks have concentrated on the effects of crystal size and stacking faults and paid little attention to the presence of expandable phases.

The present study aims to assess qualitatively the presence of such phases in high-grade diagenetic to VLGM samples and the impact of their presence on illite crystallinity measurements.

* E-mail: vali_h@geosci.lan.mcgill.ca
† Present Address: Department of Geology, Faculty of Science, Suez Canal University, Ismailia, PC. 41522, Egypt. Salah.shata@mail.mcgill.ca

FACTORS AFFECTING ILLITE CRYSTALLINITY

Variations in the illite crystallinity index may be related to several crystal-chemical and analytical factors. According to Klug and Alexander (1974), the profile of an XRD peak produced by a crystalline powder is a function of four main factors: (1) methods of sample preparation; (2) X-ray diffractometer settings; (3) crystallite size (mean size of the domains that coherently scatter X-rays, measured perpendicular to the diffracting plane) and domain-size distribution; and (4) "lattice strain" (various kinds of lattice imperfections, e.g., local heterogeneity of chemical composition and lattice structure, see below and Figs. 1d, 1e, and 1f).

The basic difficulty in drawing definite correlations among results of IC studies made in various laboratories is the lack of sufficient standardization of analytical procedures and instruments (Kisch 1990). Warr and Rice (1994) proposed a standardized scale of illite crystallinity, the crystallinity index standard (CIS), by calibrating the IC measurements according to Kisch (1991) using a set of rock-chip standards. Drits et al. (1998) summarized the findings about the importance of crystallite size. Shata (2000) reviewed the crystallite size measurements and their relation to IC and emphasized the importance of the instrumental factor for IC-measurements and extended

0003-004X/03/0506–748$05.00

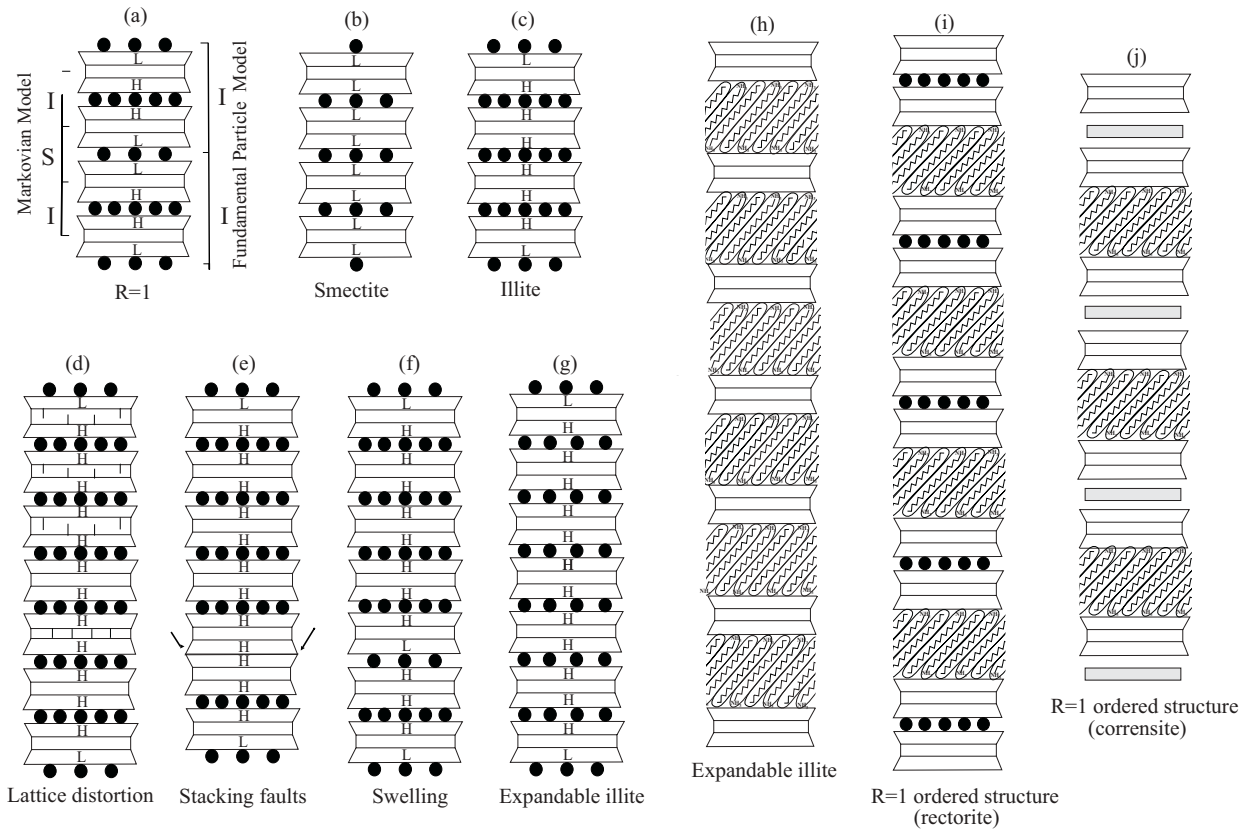

FIGURE 1. A model representing the stacking order of polar and non-polar layers in 2:1 layer-silicates (not to scale): (a) R = 1-ordered structure represented by Markovian and fundamental particle models; I = illite, S = smectite; (b) sequence of smectite layers; and (c) packet of illite. Various types of lattice imperfections (lattice strain): (d) distortion in illite lattice; (e) stacking faults including tilt (not shown); (f) presence of swelling surfaces between coherent non-expandable 2:1 layers; and (g) expandable illite model. Various 2:1 layer silicate models exhibiting expansion with $n_C = 18$: (h) expandable illite; (i) model of the R1-ordered I/V structure (rectorite); V = vermiculite; and (j) model of the R1-ordered C/V structure (corrensite); C = Chlorite. Solid circles represent relative numbers of interlayer cations, H and L stand for high and low charge within individual 2:1 layers, respectively. Diagrams a, b, and c from Vali et al. (1994).

the standardization to data processing.

Warr and Nieto (1998), among other investigators, studied ion-milled samples with the high-resolution transmission electron microscope (HRTEM) to evaluate lattice strain (ε) due to stacking faults, edge dislocations, layer terminations, and defects, which give rise to non-periodic features of the crystal structure. The samples were also characterized by XRD analyses. Expandable components have not been considered by these authors to contribute to broadening of the 10 Å XRD peak of illitic materials beyond the high-grade diagenetic zone, probably because anchizonal illite shows no reaction to glycol treatment. Smectite-group phases of prograde origin are not known to form in the anchizone. Although Merriman et al. (1990) stated that smectite is not detected in the anchizone, Merriman and Peacor (1999) in a recent review left open the question of the last occurrence of smectite in the anchizone. According to Árkai et al. (1996), expandable mixed-layers do not occur in detectable amounts in anchizonal and epizonal rocks, and thus make no significant contribution to calculation of lattice strain and crystallite-size. The continuous improvement of illite crystallinity with increasing grade is thus routinely attributed to an increase in crystallite size and a decrease in lattice strain.

We contend that the situation is more complicated. The dehydration and collapse of some smectite layers to 10 Å layers during HRTEM investigations of ion-milled I-S samples may have resulted in some ambiguity in the interpretation of the material. In other words, the presence of small amounts of expandable components (smectitic material) may have been overlooked, although Kisch (1983) already concluded that expandability is only lost at the anchizone to epizone boundary. Furthermore, high-charge expandable components cannot be differentiated from non-expandable discrete illite in both conventional XRD and HRTEM studies (Vali et al. 1991).

The aim of the present work is to evaluate the importance of expandable layers in high-grade diagenetic-VLGM samples of Lower Paleozoic sedimentary sequences in the Quebec Appalachians, and its impact on IC measurements using conventional polar interstratification compounds (e.g., solvation with ethylene glycol) and intercalation with *n*-alkylammonium ions.

MATERIALS AND EXPERIMENTAL SETTINGS

Materials and geological setting of the study area

Fifteen samples from high-grade diagenetic and VLGM terranes of the Gaspé Peninsula were chosen with the aid of IC and organic-matter maturation maps of Islam et al. (1982) and Hesse and Dalton (1991). Eight samples were taken from burial diagenetic environments; the remaining seven samples represent anchizonal conditions around the Devonian McGerrigle Mountains Pluton (Fig. 2).

The samples are argillaceous rocks from deep-water flysch deposits of the Deslandes Formation and Cap-des-Rosiers Group, forming part of the external domain of the Taconian belt of Gaspé Peninsula. According to St. Julien and Hubert (1975), the Taconian orogenic belt comprises Cambro-Ordovician sediments derived from various portions of a former passive continental margin. The younger Ordovician rocks of this belt were deposited in a foreland basin created by collision of a Late Cambrian to Early Ordovician island arc system with the passive continental margin of North America during the Taconian Orogeny. These rocks were intruded by the post-orogenic Upper Devonian–Lower Carboniferous McGerrigle Mountains Pluton, which consists of a hybrid suite of rocks ranging from syenites, granodiorites, and monzonites to gabbros in the northern part of the intrusion and earlier granitic rocks in the southern part. An exceptionally wide anchimetamorphic halo (up to 20 km wide) has been mapped around the pluton (Islam et al. 1982).

Sample preparation

The samples were separated into two size classes, a fine (<2 μm) fraction and an ultrafine (<0.1 μm) fraction. Neither grinding nor sonic or chemical treatments were used during sample preparation in order to prevent artificially generated expandability and to minimize any kind of modification of the original clay material (Wilcoxon et al. 1990). Only Na metaphosphate was added as a peptizer, where necessary. The samples were Sr-saturated in order to achieve constant thickness of the expanded structure that resulted from swelling (Eberl et al. 1987).

X-ray diffraction

For conventional measurements of expandability and IC, a concentration of >3 mg of a clay suspension/cm^2 was prepared by pipetting the suspension on to a glass slide and air-drying it at room temperature. After these untreated slides had been

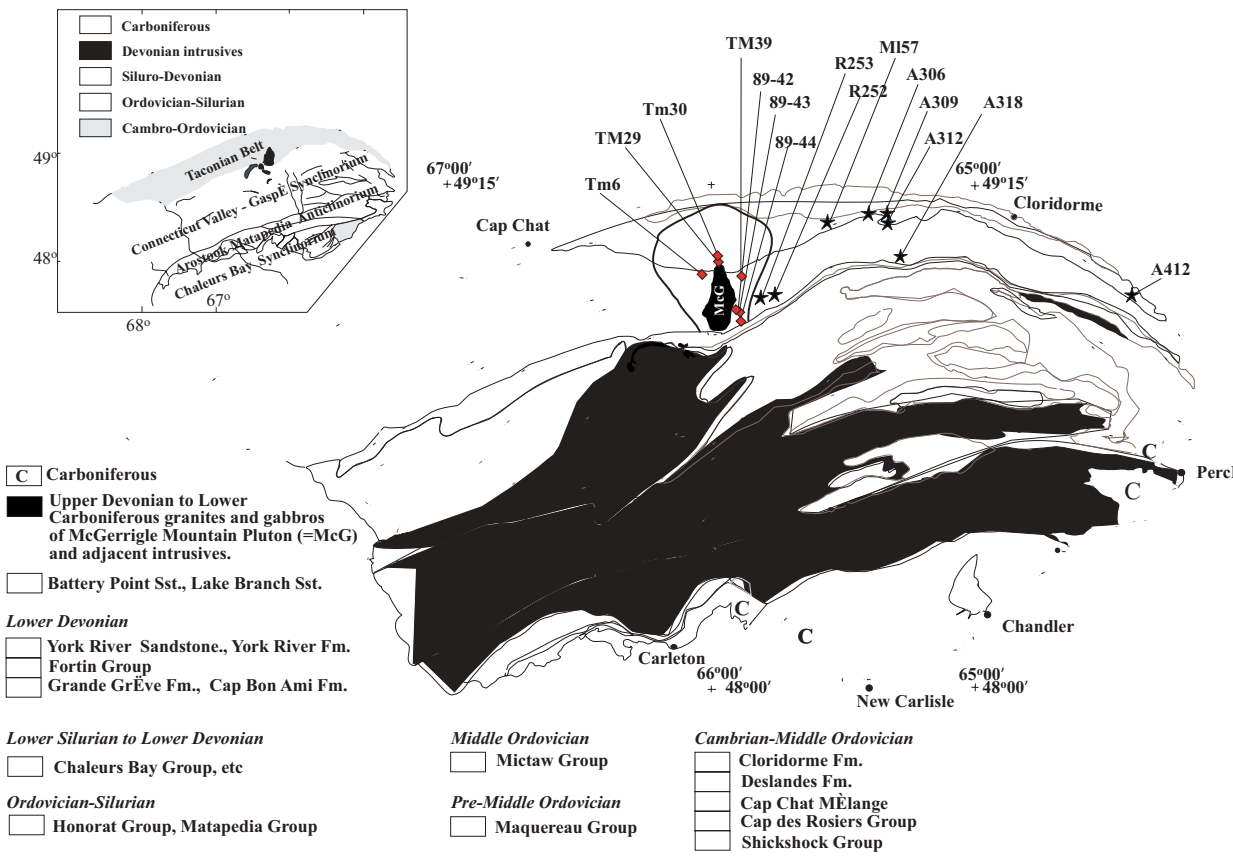

FIGURE 2. Geologic map of the Gaspé Peninsula showing the main stratigraphic units, structural elements (after Skidmore and McGerrigle 1967), and sample localities. Bold line around the McGerrigle Mountains Pluton delineates the anchizone of Hesse and Dalton (1991).

scanned by XRD, the samples were solvated with ethylene glycol (EG) under vapor pressure at 60 °C for 24 hours and immediately analyzed by XRD.

For optimum characterization of the 2:1 layer structure and for detection of expandability, the clay fraction was intercalated with octylammonium ions ($n_C = 8$) and octadecyl-ammonium ions ($n_C = 18$), where n_C is the number of carbon ions per alkyl chain. Shorter ($n_C = 8$) ions are used for their ability to differentially expand low- and high-charge expandable 2:1 clay minerals, whereas the $n_C = 18$ ions selectively deplete interlayer K from illitic and micaceous phases (Vali and Hesse 1992). By substituting for interlayer K and other cations from a wide range of micas, such as illite, glauconite, and the high-charge variety of I-S mixed-layers, $n_C > 12$ ions expand these phases. High-charge I-S mixed layers do not respond to ethylene glycol or glycerol and do not expand upon treatment with $n_C < 12$ (Vali et al. 1991, and references therein). In contrast, smectite-group phases and vermiculite react with short and intermediate alkylammonium cations ($6 \leq n_C \leq 11$) as well as long chains (Vali et al. 1992).

For *n*-alkylammonium intercalation, 50 mg of freeze-dried clay were incubated at 65 ºC in glass centrifuge tubes with 10 mL of the appropriate solution of *n*-alkylamine hydrochloride (using a 0.5 N solution for octylamine hydrochloride and a 0.05 N solution for octadecylamine hydrochloride, respectively) for five days. The details of the intercalation and washing process are given in Rühlicke and Kohler (1981) and Lagaly (1994). The *n*-alkylammonium clays were dispersed in a 1:1 90% ethanol-deionized H_2O solution, pipetted onto glass slides, and allowed to dry at room temperature. Then the slides were placed overnight in a freeze-dryer under high vacuum (in order to prevent incorporation of alcohol with the *n*-alkyl ammonium ion inside the 2:1 layer silicate) and immediately taken to the diffractometer.

XRD analysis was carried out on a 12 kW rotating anode Rigaku D/Max 2 automated powder diffractometer equipped with a graphite diffracted-beam monochromator (Cu*K*α radiation) and a theta compensating slit assembly. The system was operated under the following analytical conditions: voltage of 40 kV, beam current of 100 mA, step-size of 0.01° 2θ, counting time of 1 second per step, 0.15 mm receiving slit, and a scanning range of 2 to 40 °2θ. The proportion of expandable interlayers and type of order of illite-smectite (IS) mixed-layers were estimated from the experimental XRD patterns of Mg-saturated and EG-solvated samples or samples intercalated with $n_C = 8$ and $n_C = 18$ using the Δ2θ method of Moore and Reynolds (1997). Środoń's (1984) intensity ratio $Ir = [I(001)/I(003)]_{air\text{-}dried}/[I(001)/I(003)]_{glycolated}$, which is very sensitive to the presence of swelling layers in illite, was not applicable due to the presence of fine-grained quartz in almost all samples.

High-resolution transmission electron microscopy

HRTEM combined with *n*-alkylamonium treatment allows distinction between expanded and non-expanded interlayers in interstratified structures under the electron beam and thus becomes a critical tool to document the evolution of 2:1 clay minerals in high-grade diagenetic and VLGM environments.

The 2:1 clay mineral samples (dehydrated with polypropylene) were embedded in a low-viscosity, thermally curing epoxy resin (Spurr 1969) for preparation of ultrathin sections following the method of Vali and Köster (1986). Ultrathin sections were transferred to 1.5 mL microtest tubes containing 1.0 mL of the *n*-alkylammonium-cation solution diluted to 40–50% of the initial concentration (Vali and Hesse 1990).

All ultramicrotomed samples were imaged in bright-field illumination at high resolution with a JEOL JEM-100 CX II transmission electron microscope (TEM) at an accelerating voltage of 100 kV. TEM imaging was performed with focus conditions approximating the Scherzer defocus (underfocus) depending on the structure and thickness of the specimen and instrumental conditions (Vali et al. 1991; Vali and Hesse 1992). Under these conditions, dark fringes approximately overlie regions of relatively high density (2:1 layer silicate), and bright fringes approximately overlie regions of relatively low density (interlayers). Because the work depends critically on transmission electron microscopy, we start with a TEM-based definition of 2:1 layer silicates.

TEM-BASED DEFINITON OF 2:1 LAYER SILICATES

Vali et al. (1994) concluded from HRTEM studies combined with XRD that smectite-group phases, vermiculite, and "expandable illite" all consist of polar 2:1 layers, whereas packets of illite consist of interior non-polar layers and exterior polar layers. In an interior non-polar layer, the surfaces on both sides of individual 2:1 layers have the same charge density, i.e., the isomorphous substitution in the individual layers of tetrahedral, octahedral, and tetrahedral (T-O-T) sheets is symmetrical (Figs. 1b and 1c). A rectorite-like, R1-ordered phase is composed of polar 2:1 layers only (Fig. 1a), and considered to be a single phase (Lagaly 1979; Ahn and Peacor 1986).

DETECTION OF EXPANDABILITY: N-ALKYLAMMONIUM INTERCALATION VS. GLYCOLATION

Expandability (conventionally defined as %S layers in mixed-layer I-S) is a fundamental parameter to assess the evolution of phyllosilicates during diagenesis and VLGM. Expandable clay minerals like those of the smectite group occur as a component of mixed-layer clays in argillaceous sediments. During burial diagenesis, the percentage of expandable layers in mixed-layer clays decreases systematically as a function of many factors; chief among them is temperature (burial depth) (Środoń and Eberl 1984). Below 10–20% S, expandable components become difficult to detect with conventional methods. For samples formed under high-temperature conditions (>165 °C), EG solvation causes only a slight sharpening (or none at all) of the reflections (Hunziker et al. 1986; Yang and Hesse 1991). A few abnormal samples in the Gaspé suite show slightly wider and weaker XRD peaks that shift to higher 2θ angle upon glycolation. The reason for these changes is not fully understood, but is presumably due to loosening of the structure by the penetration of EG along the boundaries of the relatively large, ordered crystallites (coherently scattering domains).

The conventional methods to assess expandability, such as the shift in the peak position of glycolated samples ($\%S_{XRD}$, Środoń 1981) or the intensity ratio [$Ir = I(001)/I(003)_{air\text{-}dried}/I(001)/I(003)_{glycol}$, Środoń 1984] are no longer suitable under

anchizonal conditions (discussed below). In ion-thinned samples studied under the HRTEM, expandable components cannot be detected because they collapse in the high vacuum under the electron beam. It is for these reasons that the role of expandable components in high-grade diagenetic and VLGM rocks has remained obscure and poorly documented.

The limitations and ambiguities of glycolation as a means of assessing expandability in XRD patterns were discussed by Ransom and Helgeson (1989). Glycolation does not differentiate between low-charge vermiculite and high-charge smectite. Furthermore, neither high-charge vermiculite nor expandable illite respond to glycolation.

The occurrence of different types of expandable components and, consequently, of variations in interlayer-charge density can be detected by XRD and HRTEM in *n*-alkylammonium-treated samples, whereas ethylene glycol treatment of XRD mounts is indifferent to these variations. The arrangement of alkylammonium ions exchanged for inorganic interlayer-cations in smectite, vermiculite, illite, and mixed-layer minerals and the degree of expansion are a function of alkyl chain length ($6 \leq n_C \leq 18$) and the density of interlayer charge (see Appendix).

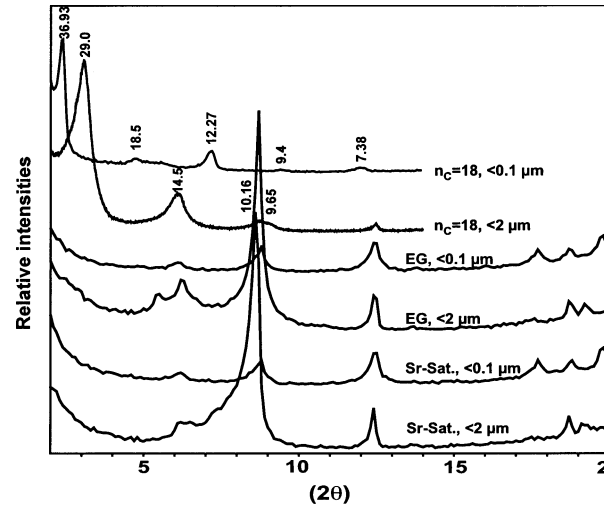

FIGURE 3. XRD patterns of sample TM39 (Cap-des-Rosiers Group, McGerrigle Mountains Pluton anchizone, Gaspé Peninsula) showing the response of different size fractions to glycolation and alkylammonium ion intercalation. Sr-Sat stands for air-dried, Sr-saturated; EG = ethylene glycol; n_C = 8, octylammonium cations; n_C = 18, octadecylammonium cations.

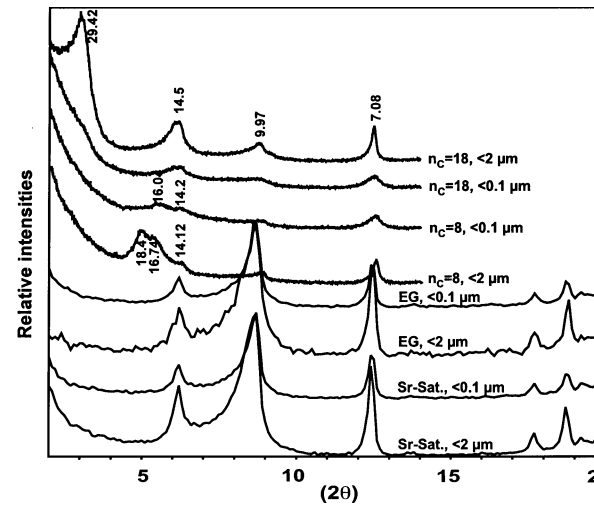

FIGURE 4. XRD patterns of sample TM29 (Deslandes Formation, McGerrigle Mountains Pluton anchizone, Gaspé Peninsula) showing the response of different size fractions to glycolation and alkylammonium ion intercalation (same abbreviations as in Fig. 3).

RESULTS: XRD CHARACTERIZATION OF GLYCOLATED AND N-ALKYLAMMONIUM INTERCALATED ILLITIC AND CHLORITIC MATERIALS

FWHM of the 10 Å diffraction peak

Air-dried, high-grade diagenetic samples show a fairly broad asymmetrical basal (001) diffraction peak at 10 Å. After glycolation the 10 Å peak shifts slightly toward a higher 2θ angle, indicating the presence of expandable layers. On the other hand, the FWHM of the 10 Å peak narrows within the high-grade diagenetic zone and in the transition to the anchizone and further in that zone with increasing grade, indicating some structural modification. Anchimetamorphic illite of Gaspé Peninsula shows no significant XRD-shift upon glycol treatment (Figs. 3 and 4), and behaves similarly to the phyllosilicates in the diagenetic and VLGM zones of the Glarus Alps, Switzerland (Hunziker et al. 1986), and of the southern Quebec Appalachians (Yang and Hesse 1991). The details of the behavior of the 10 Å difraction peaks of illitic phases of Gaspé Peninsula phyllosilicates with glycolation in both the fine and ultrafine fractions are given in Table 1 and Figs. 3, 4, 8, and 9.

A few samples show abnormal behavior upon glycolation. The XRD peaks become slightly wider and weaker, and shift to higher 2θ angles.

Peak positions and peak intensities

Besides being affected by domain size distribution, mineral composition, and machine effects, the position and intensity of peaks in the XRD patterns of illitic materials are principally related to swelling characteristics, which strongly depend on the mixed-layer content. In the few cases where detrital quartz was absent, the intensity ratio $Ir = [I(001)/I(003)]_{\text{air-dried}} / [I(001)/I(003)]_{\text{glycolated}}$ (Środoń 1984) failed to detect the presence of expandable layers in high-grade diagenetic and VLGM rocks because the samples did not respond (or responded anomalously) to EG (i.e., showed *Ir* values <1), suggesting that the Środoń intensity ratio is not a sensitive parameter in anchizonal or higher-grade rocks.

Intercalation with *n*-alkylammonium cations

The expandability of illite in anchizonal samples was evaluated by comparing lattice-fringe images of 2:1 clay minerals in the <2 μm and <0.1 μm fractions before and after treatment with short- and long-chain alkylammonium cations with their

XRD patterns (glycolated and untreated samples). The response of illite to n-alkylammonium intercalation is different in high-grade diagenetic and anchizonal samples (Table 1) and is used to identify the various 2:1 clay mineral components and their expansion properties on the basis of their *d*(00*l*) values (Figs. 3 and 4). No quantification of the expandability is attempted at this stage, although the tools used in this study certainly have the potential to quantify low concentrations of expandable phases in mixed-layer clays, and this is a high priority for future research.

Following is the description of the HRTE micrographs together with the XRD data and suggested models for the 2:1 layer silicates present.

COMPARISON OF XRD RESULTS WITH HRTEM CHARACTERIZATION OF INDIVIDUAL PHASES

Expandable illite with abundant double layers and packets of non-expandable illite

Illite and some varieties of mica possessing interlayers intercalated with $n_C = 18$ in a paraffin-type arrangement generally have a *d*(001) of 29 to 31 Å (e.g., a ~10 Å 2:1 layer silicate + a 19 Å $n_C = 18$ expanded interlayer, Figs. 1g and 1h) in XRD, whereas in HRTEM images, *d*(001) is measured as ~24–25 Å (~10 Å silicate layer + ~14 Å intercalated $n_C = 18$ interlayer). The difference in the *d*-values may be due to radiation damage of the alkylammonium ions (evaporation of ammonia) under the electron beam in TEM (Vali and Hesse 1990; Vali et al. 1991).

In all samples of high-grade diagenetic and VLGM rocks of the Gaspé suite, illite coexists with chlorite (Shata and Hesse 1998). Vali et al. (1991) reported that expandable illite is represented by a set of integral reflections having *d*-values of 30, 15, and 10 Å (as documented in the present study, Fig. 3). The second and the third reflections of expandable illite may be superimposed on the sharp basal reflections of chlorite and illite, respectively. This superposition may explain the broadening of the first two basal reflections of chlorite after $n_C = 18$ intercalation (Fig. 3), although lattice-fringe images do not show expandable chlorite phases (except for samples A309 and A312).

Expandable illite forms the main constituent of most of the <2 μm fractions of the Gaspé samples. Treatment with long-chain alkylammonium cations ($n_C \geq 12$) produced two characteristic XRD reflections, a 10 Å peak representing non-expandable illite (packets of discrete non-expandable 2:1 layer silicate in HRTEM) and a 29–31 Å peak (uniform coherent expandable 2:1 layers of 25 Å spacing in HRTEM) representing highly charged "expandable illite" (Fig. 5). We prefer to retain the original descriptive name "expandable illite" suggested by Laird et al. (1987) and Vali et al. (1991) for illitic material containing intercalated alkylammonium cations with a paraffin-type arrangement in the interlayers rather than using n-alkylammonium illite, the name introduced by Sears et al. (1998).

Vermiculite

Only one sample (TM29) exhibits an expansion in response to $n_C = 8$ as well as to $n_C = 18$ intercalation. The sample is characterized by three sharp XRD reflections, at 29.4, 14.5, and 9.97 Å after $n_C = 18$ treatment, whereas it expanded to 18.6 Å upon intercalation with $n_C = 8$ (in contrast to expandable illite, which does not expand in response to $n_C = 8$). This material may be interpreted as intermediate- to high-charge vermiculite with a paraffin-type arrangement of the alkyl chains (compare the glycolated and $n_C = 18$-treated patterns in Fig. 3). Another distinction between expandable illite and vermiculite is the absence of a 10 Å peak after treatment with $n_C = 18$. In other words, vermiculite is responding thoroughly to $n_C = 18$ intercalation, whereas expandable illite exhibits selective expansion, retaining packets of non-expanding illite that give rise to the 10 Å peak.

Lattice-fringe images for this sample (TM29) show a coherent pattern of fully expandable interlayers with a uniform spacing of 25 Å (Fig. 6) alternating with a few very thin non-expandable 10 Å 2:1 layers.

Rectorite-like R1-ordered 2:1 layer-structure

The XRD pattern of the samples containing this phase is characterized by a sharp peak at 36.2–36.9 Å along with a set of integral reflections (e.g., Fig. 3). The pattern is attributed to an R1-ordered structure characterized by a superstructure with a set of approximately integral reflections 36.9 (001)*, 18.5 (002)*, 12.3 (003)*, 9.4 (004)*, and 7.38 (005)* Å. Vali and Hesse (1992) attributed similar integral reflections at 36, 18, and 12 Å in the Jefferson vermiculite treated with $n_C = 18$ to vermiculite itself. They related the additional expansion to the effects of ethanol, a polar molecule used in the washing steps that may aggregate to form clusters between the alkyl chains (Lagaly 1987). In the present study, any expansion due to the presence of ethanol was excluded by placing the slides overnight in a freeze-dryer under high vacuum and then immediately scanning them.

Lattice-fringe images of the rectorite-like phase shows two different responses of the 2:1 layer-structure to $n_C = 18$ intercalation. In Figure 7, the main domain consists of more than 40 double layers with expandable interfaces of 26–27 Å spacing and eight packets of non-expandable 2:1 layers ranging in thickness from 5 to 29 2:1 layers.

The R1-ordered structure consists of one non-expandable 2:1 silicate layer (10 Å) and one 2:1 silicate layer with an $n_C =$ 18 expanded interlayer of 27 Å (10 + 27 = 37 Å). The intercalated $n_C = 18$ interlayer suggests an intermediate to high interlayer charge-density typical of vermiculite with a paraffin-type arrangement of the alkyl chains (Figs. 1i and 3). The phase seems to be confined to the anchizonal samples, either in the < 2 μm (sample 89-44) or in the <0.1 μm fraction (samples TM30 and TM39). Furthermore, the same R1-ordered structure was found in the fine fraction of burial diagenetic material (samples A309 and A318), but with one major difference: the XRD pattern of the $n_C = 18$ intercalated sample gives an integral set of reflections, 34.5–17.2–11.5 Å (Fig. 8). An R1-ordered structure of rectorite may thus still exist in burial-diagenetic and VLGM terranes, with the expandable interlayer charge being higher in VLGM than in the burial diagenetic zone.

Corrensite-like R1-ordered layer structure

The XRD pattern of the treated material is characterized by a sharp 43–44 Å peak along with a set of integral reflections.

TABLE 1. Illite crystallinity (FWHM) and XRD peak position of <2 μm and <0.1 μm fractions of *n*-alkylammonium (n_c = 18) intercalated samples

Diagenetic grade	Burial diagenesis						
Stratigraphy	Deslandes Fm					Cap des-Rosiers Gp.	
Sample no.	A306*	A309	A312	A412	ML57	A318	R252
				FWHM*			
<2 μm	0.395–0.345	0.547–0.504	0.545–0.5.4	0.413–0.426	0.342–0.298	0.379–0.421	0.306–0.302
<0.1 μm	0.273–0.311	0.291–0.335	0.504–0.478	0.401–0.669	0.328–0.303	0.295–0.440	0.307–0.368
				XRD peak positions of n_c = 18 intercalated samples in angstroms			
<2 μm	[44.1, 21.9][a]	[30.7, 15.2,10.3][b]	[31, 15.01, 10.2][g]	[30][b]	[23.58, 17.7, 15.35 11.8, 10.06][h]	[29.7, 14.81, 9.9][b]	[30.2, 15, 10.1][b]
<0.1 mm		[(51.3, 17.1, 10.3,[c]) (14, 7) (34.5, 17.2, 11.5)[e]][f]				[(44.4, 22.3, 14.8, 11.18, 8.94, 7.45)[i], (34.3, 17.72, 11.4, 8.3)[e]]	[(42.0, 20.8, 14.3, 10.5, 8.40)[i]][j]

* Air dried glycolated.

Notes on XRD expansion (in angstroms) due to n_c = 18 treatment:

[a] Expandable phase occurs only in <2 μm fraction represented by small shoulder at 44 Å and very wide hump at 5–6° 2θ. Fine fraction gives very diffused XRD-pattern.

[b] Expandable illite.

[c] R3-ordered layer structure.

[d] The 14 and 7 Å peaks becomes very broad.

[e] Rectorite-like R1-ordered 2:1 layer-structure.

[f] Where there is more than one phase in a give sample, peak positions for individual phases are shown in parentheses and grouped by square brackets.

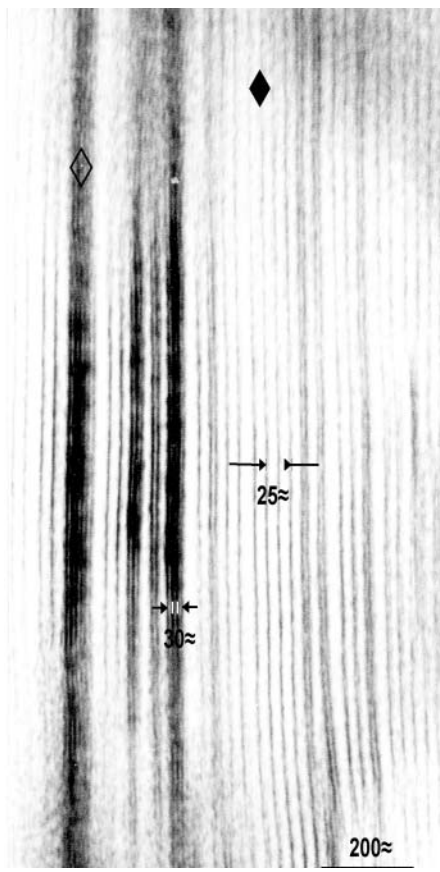

FIGURE 5. HRTEM image of the <2 μm size-fraction of sample TM39 from the McGerrigle Mountains Pluton anchizone after treatment with n_C = 18 showing coherent packets of expandable illite with average spacing of 25 Å (solid diamond) alternating with thin packets of non-expandable 2:1 layers with 10 Å spacing (open diamond).

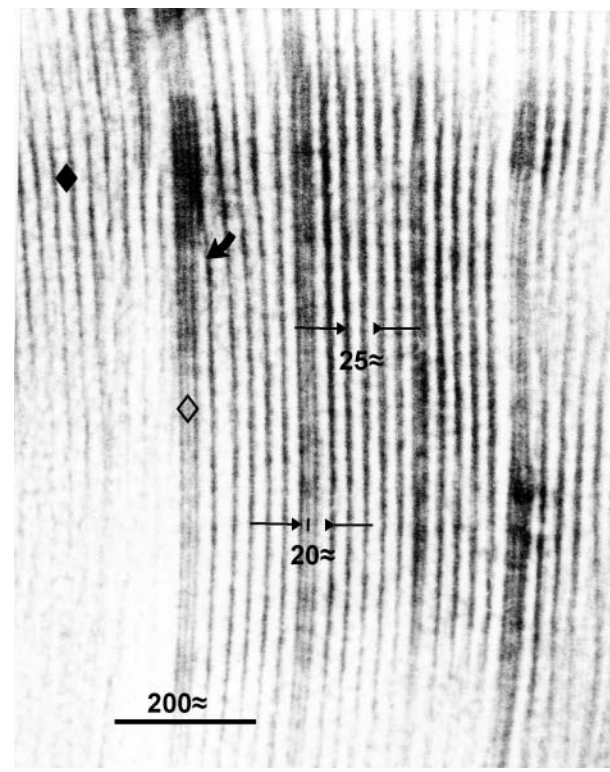

FIGURE 6. HRTEM image of the <2 μm size-fraction of sample TM 29 from the McGerrigle Mountains Pluton anchizone after treatment with n_C = 18 showing coherent packets of expanding 2:1 layers with average spacing of 25 Å (solid diamond) alternating with very thin packets of two to three 2:1 layers of "non-expandable illite" (open diamond). The solid arrow indicates the non-expandable packet termination and conversion to a fully expanded coherent domain.

TABLE 1. —Expanded.

Burial diagenesis	McGerrigle anchizone				
Cap des-Rosiers Gp.	Cap des-Rosiers Gp.			Deslandes Fm	
R253	89-44	TM6	TM39	TM29	TM30
FWHM*					
0.440–0.490 0.290–0.340	0.354–0.413 0.480–0.559	0.314–0.303 0.303–0.289	0.360–0.495 0.509–0.351	0.627–0.609 0.434–0.555	0.262–0.29 0.561–0.469
XRD peak positions of n_c = 18 intercalated samples in angstroms					
[31.53, 15.9, 10.5][b] [43.9, 22.2, 14.8, 11.1)[i]][k]	[36.2, 17.92, 11.96][e]	[22.1, 17.2][l]	[29][b]	[29][m]	[31, 15.5, 10.3][b]
[(51.62, 25.8, 17.2, 10.4)[c], [43.7, 21.5, 14.6][l] (34.5,17.2,11.5)[e], (44.4, 22.3, 14.9, 11.1, 8.9)[i]		[17.13, 11.04, 6.2][l]	[36.9, 18.5, 12.2, 9.36][e]	[29][m]	[(43.6, 21.55, 14.5)[j] (35.6, 17.88, 12.04)[e], [51.2, 17.1, 12.8, 10.4)[c]

[g] Expandable illite in both <2 μm and <0.1 μm fractions.
[h] <2 μm fraction: 10 Å peak little affected, <0.1 μm: only very broad peaks at 23.8, 15.3, 11.7 Å.
[i] Corrensite-like R1-ordered layer structure.
[j] Peak broadening in the fine fraction not related to expandable component.
[k] The main phase is corrensite (44 Å); expandable illite (31 Å) is represented only by a shoulder.
[l] Expandable phase in both <2 μm and <0.1 μm fractions represented by very weak, broad peak compared to glycolated samples. Both fractions do not respond to n_C = 8
[m] Both fractions expand to 29 Å with n_C = 18, but are interpreted as vermiculite because they respond also to n_C = 8.

The diffraction peak at 44.4 Å (001)* suggests a superlattice reflection with a set of the integral higher-order reflections of 22.2 (002)*, 14.8 (003)*, 11.1 (004)*, 8.9 (005)*, 7.4 (006)*, 6.4 (007)* Å (Figs. 8 and 9). The pattern is attributed to a corrensite-like, R1-ordered 2:1 layer structure.

Lattice-fringe images of sample R253 treated with n_C = 18 (14 Å) and one 2:1 layer silicate with n_C = 18 expanded interlayers of 29–30 Å, yielding a superstructure reflection of 43 to 44 Å. The intercalated n_C = 18 interlayer suggests a high charge-density typical of vermiculite, with a paraffin–type arrangement of the alkyl chains.

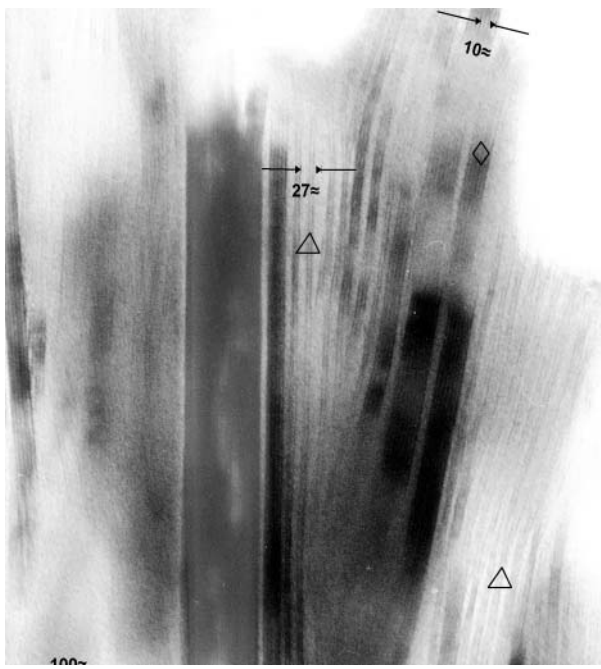

FIGURE 7. HRTEM images of the <0.1 μm size-fraction from the McGerrigle Mountains Pluton anchizone (sample TM 39) after treatment with n_C = 18: Sequence of an R1-ordered structure consisting of double layers having expandable interfaces with an average spacing of 27 Å (vermiculite, open triangle) and thick packets of 2:1 layer-silicates with non-expandable interlayers (10 Å, open diamond).

According to Bailey et al. (1982), corrensite may be defined as regular interstratification of trioctahedral chlorite with either trioctahedral smectite or trioctahedral vermiculite. The former is called "low-charge corrensite" whereas the latter is called "high-charge corrensite." Shau et al. (1990) recommended that corrensite be treated as single phase rather than a 1:1 ordered mixture. Corrensite is widespread, and found in various environments. It has been previously documented in high-grade diagenetic (Wybrecht et al. 1985) and in VLGM rocks (e.g., Dunoyer de Segonzac 1970; Jiang and Peacor 1994; Dalla Torre et al. 1996).

Like the rectorite-like, R1-ordered layer structure, the chlorite mixed-layers are abundant in the fine fractions of Gaspé samples, with the exception of sample R253 (<2 μm). The corrensite-like, R1-ordered structure occurs in burial diagenetic and VLGM rocks, mostly those of the Cap-des-Rosiers Group. Its origin may be provenance-related and thus reflect a detrital origin. The XRD patterns of these samples do not respond to glycolation, probably because the expandable component has a high density of interlayer charge. Also, the expandable interlayers may be isolated between illite clusters; their contribution to the XRD-measurable expandability is considered to be minor.

"Kalkberg" R3-ordered layer structure

An R3-ordered 2:1 layer-structure consists of three 10 Å 2:1 layers (30 Å) and one 2:1 layer with an n_C = 18-expanded interlayer of ~22 Å. The intercalated n_C = 18 interlayer suggests the presence of an intermediate interlayer charge-density typical of vermiculite with a paraffin-type arrangement of the n_C = 18 cations. This proposal is in agreement with the findings

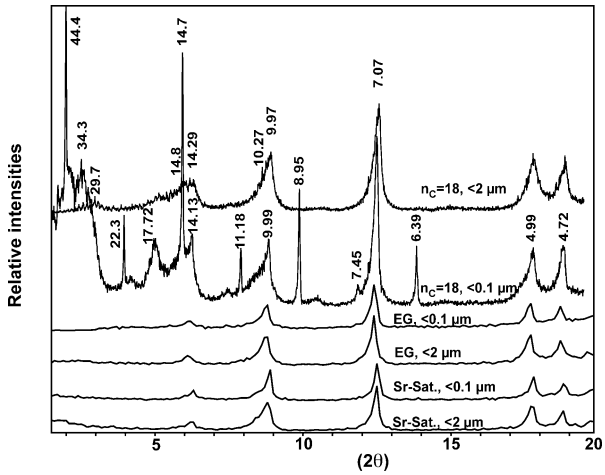

FIGURE 8. XRD patterns of sample A318 (Cap-des-Rosiers Group, burial diagenetic zone, Gaspé Peninsula) showing the response of different size fractions to glycolation and alkylammonium-ion intercalation (same abbreviations as in Fig. 3).

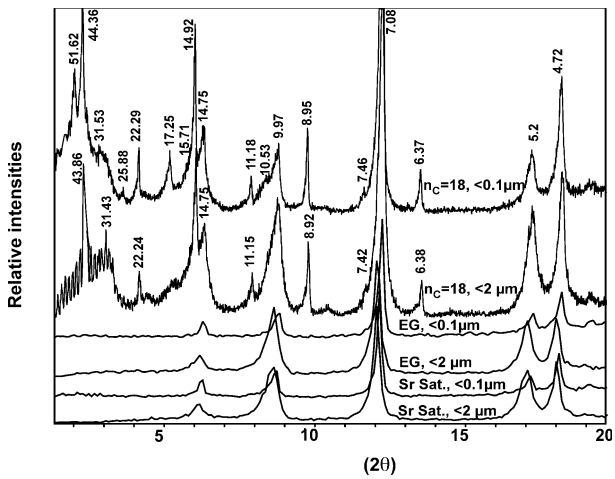

FIGURE 9. XRD patterns of sample R253 (Cap-des-Rosiers Group, burial diagenetic zone, Gaspé Peninsula) showing the response of different size fractions to glycolation and alkylammonium-ion intercalation (same abbreviations as in Fig. 3).

of Cetin and Huff (1995) that the expandable interfaces of illite-rich I-S have a vermiculite-like charge-density of the interlayer.

The XRD pattern of sample R253, treated with $n_C = 18$, is dominated by a series of sharp reflections between 2 and 12° 2θ (Fig. 9). In addition to expandable illite and a corrensite-like structure, a superlattice structure found in the fine fraction of this sample produces a set of integral reflections of 51.6 (001)*, 25.8 (002)*, 17.2 (003)* and 10.4 Å (005)* (Fig. 9). These peaks are attributed to an R3-ordered structure.

Lattice-fringe images of the <0.1 µm fraction of sample R253 after treatment with $n_C = 18$ show 2:1 clay minerals forming sequences of packets having between 3 to 6 non-expandable 2:1 layers, with single expandable interlayers between

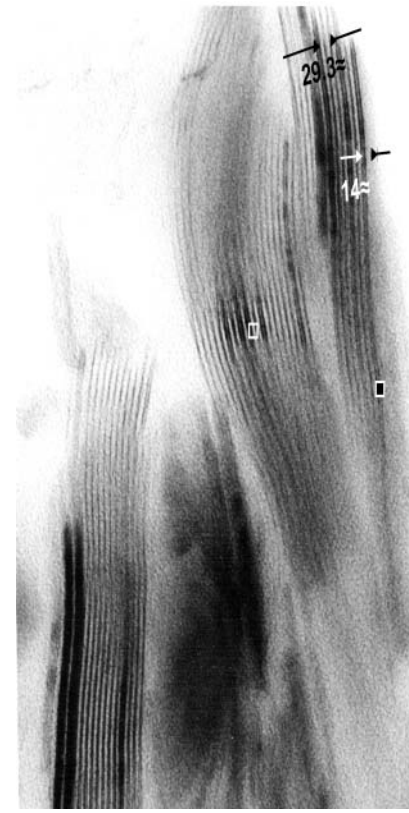

FIGURE 10. HRTEM images of the <0.1 µm size fraction from the McGerrigle Mountains Pluton anchizone (sample TM39) after treatment with $n_C = 18$ showing a sequence of a corrensite-like, R1-ordered structure consisting of double layers, alternating between non-expandable 14A 2:1 layers (solid squares) and expandable interlayers with average spacing of 29–30 Å (open squares).

adjacent packets (Fig. 11). This R3-ordered structure is stacked in a coherent sequence.

The occurrence of an R3-ordered layer-structure in the phyllosilicates of the Gaspé suite is consistent with the observation of Krekeler and Huff (1993) that corrensite and R3-ordered I-S coexist. They cited the Middle Ordovician K-saturated bentonite from the Hamburg Klippe, central Pennsylvania, as an example that has a VLGM origin.

Discrete illite and chlorite

The ultrafine (<0.1 µm) fractions of both high-grade diagenetic and VLGM samples in the Gaspé suite comprise thin packets of discrete, non-expandable 2:1 layer-silicates (Fig. 12) along with expandable phases. In contrast, the <2 µm fractions exhibit thick packets of an illitic or micaceous phase, either present as expandable illite or as non-expandable discrete illite. The latter is restricted to the <2 µm size-fractions. The lattice-fringe image in Figure 13 shows three very thick parallel domains ranging in thickness from 20 to 30 2:1 layers, with non-expandable interfaces. All three domains show phase contrast (mottled appearance), which may be interpreted as being due to lattice strain, unless it is an artifact (due to a change in

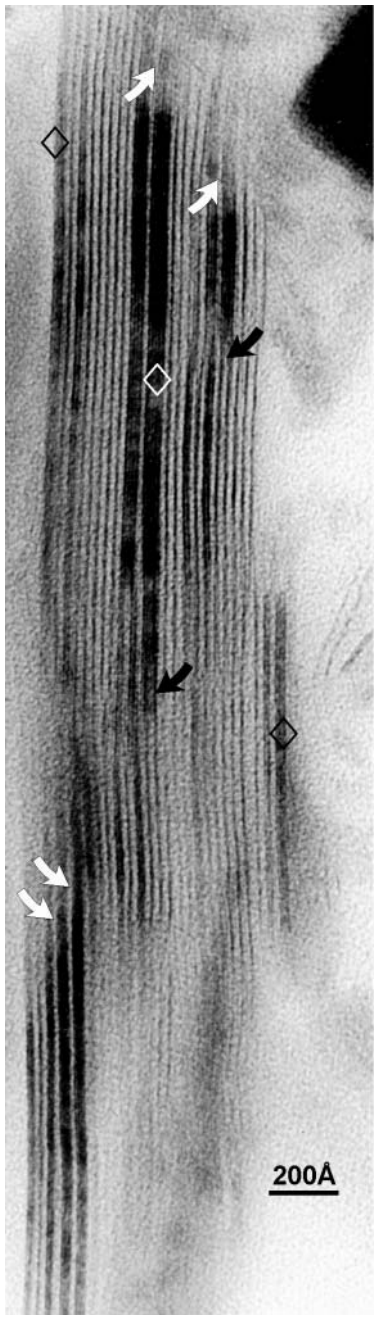

FIGURE 11. HRTEM image of the <0.1 µm size-fraction from McGerrigle Mountains Pluton anchizone (TM 39) after treatment with n_C = 18 showing R3-ordered structure consisting of thin packets of 3 to 6 non-expandable layers (open diamond with expandable interface with an average spacing of 21–22 Å (white arrows). The black arrows denote the termination of non-expandable packets and conversion to a fully expanded coherent domain.

FIGURE 12. HRTEM image of the <0.1 µm size fraction from burial-diagenetic sample A312 (Deslandes Formation) after treatment with n_C = 18 showing abundant small short packets of non-expandable 2:1 layers (illite, open diamonds) occurring together with small packets of expandable illite (solid diamond).

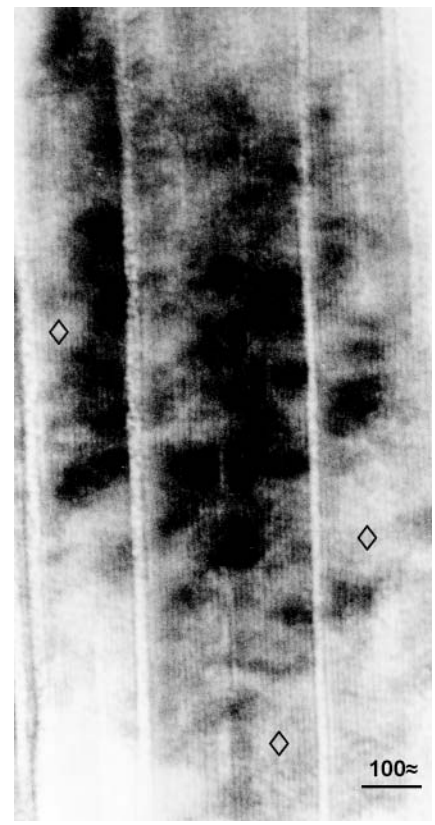

FIGURE 13. HRTEM image of the <2 µm size-fraction of sample 89-44 from the McGerrigle Mountains Pluton anchizone (Cap-des-Rosiers Group) after treatment with n_C = 18 showing a sequence of three very thick domains of non-expandable 2:1 layer (open diamonds).

thickness or sample tilt of the ultra-thin section). Furthermore, chlorite forms very thick packets (>35 2:1 layers) in the coarse fractions (Fig. 14).

In addition to the ordered mixed-layer phases, non-ordered, random expansion also exists under high-grade diagenetic and VLGM conditions in the Gaspé suite (Fig. 15). In some cases, a discrepancy between XRD and HRTEM results of *n*-alkylammonium-treated clays can be observed. For example, in the XRD pattern of the <2 µm fraction of sample TM39 (Fig. 3), only the presence of expandable illite can be detected, whereas the lattice-fringe image (Fig. 16) indicates the pres-

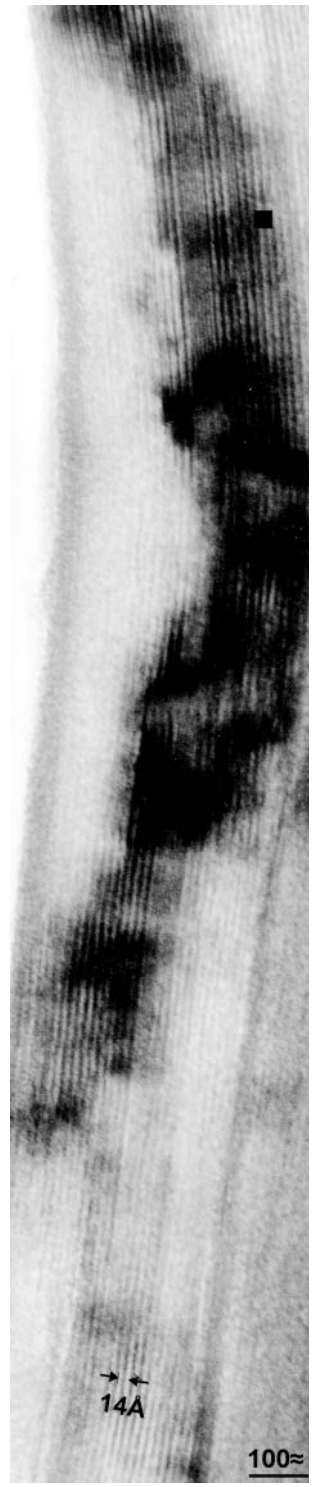

FIGURE 14. HRTEM image of the <2 μm size-fraction of sample TM6 from the McGerrigle Mountains Pluton anchizone (Cap-des-Rosiers Group) after treatment with n_C = 18 showing very thick domains of non-expandable 2:1 layer silicates (chlorite, solid square).

ence of non-expandable packets and rectorite-like R1-ordered layers, in addition to expandable illite, as well as a few packets of randomly expanded mixed layers. This discrepancy may be due to the minor proportion of the additional ordered phases, or it may be caused by overlap of XRD peaks.

INTERPRETATIONS AND DISCUSSION

The present study successfully demonstrates the presence of expandable components in high-grade diagenetic and anchizonal samples. This demonstration rests on HRTEM images and on the relationship to IC. However, such components at this grade are considered metastable and will ultimately disappear rapidly during prograde recrystallization.

Disapparance of expandable components

With prograde changes in the VLGM zone, expandability is expected to reach a minimum, beyond which stacking faults may be the main cause of peak broadening (or imperfect crystallinity). Consequently, the continuous sharpening of the 10 Å X-ray reflection in a prograde alteration sequence in anchizonal rocks is interpreted as gradual conversion of the last remaining expandable phases to illite, to the point that stacking faults remain the dominant factor causing imperfect crystallinity. In other words, peak broadening in the diagenetic zone and the low-grade anchizone is mainly attributed to the presence of expandable components. Under these conditions, the size of coherently diffracting domains increases, and the lattice distortions decrease. In the epimetamorphic zone, where expandibility has reached a minimum, stacking faults may then become the main or sole source of lattice distortion. Lattice distortion in epizonal rocks seems to reflect mechanical deformation, as it is common in kink bands and in the vicinity of dislocations (L.N. Warr, pers. comunication 2001). At this stage, the lattice distortion bears no systematic relation to the mean illite crystallite size (Árkai and Tóth 1983; Shata 2000).

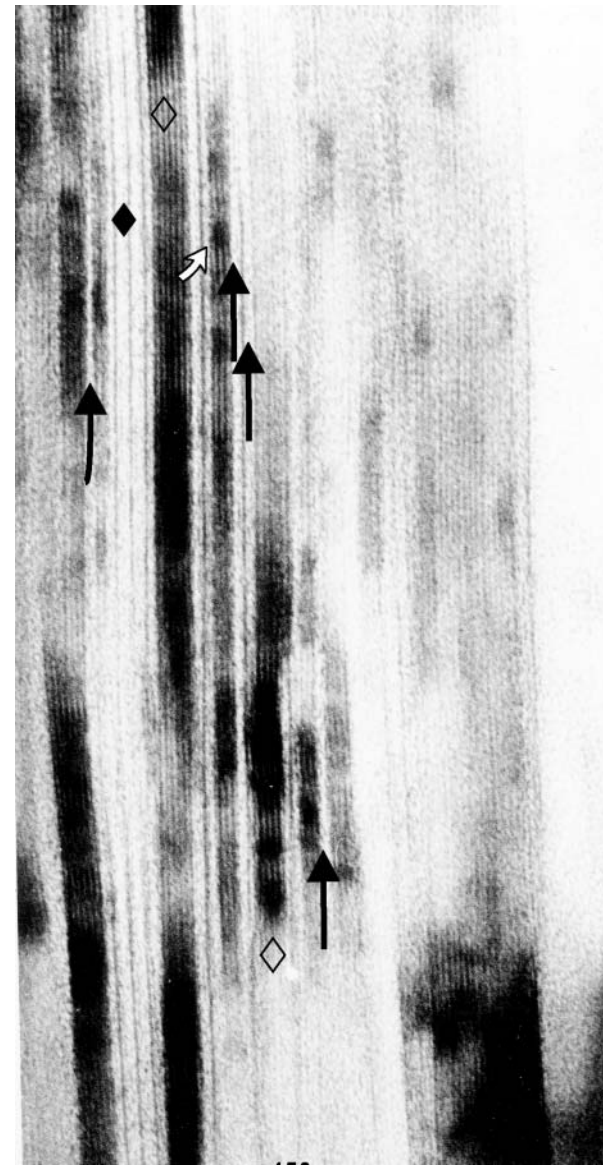

FIGURE 15. HRTEM image of the <2 μm size fraction from the Cap-des-Rosiers Group, McGerrigle Mountains anchizone (sample TM6) after treatment with n_C = 18 showing the existence of random expansion of illitic material (long solid arrow), abundant packets of non-expandable illite (open diamonds) alternating randomly with expandable illite (solid diamonds), and R3-ordered structure (white arrow, pointing to the expandable interface of the R3 structure).

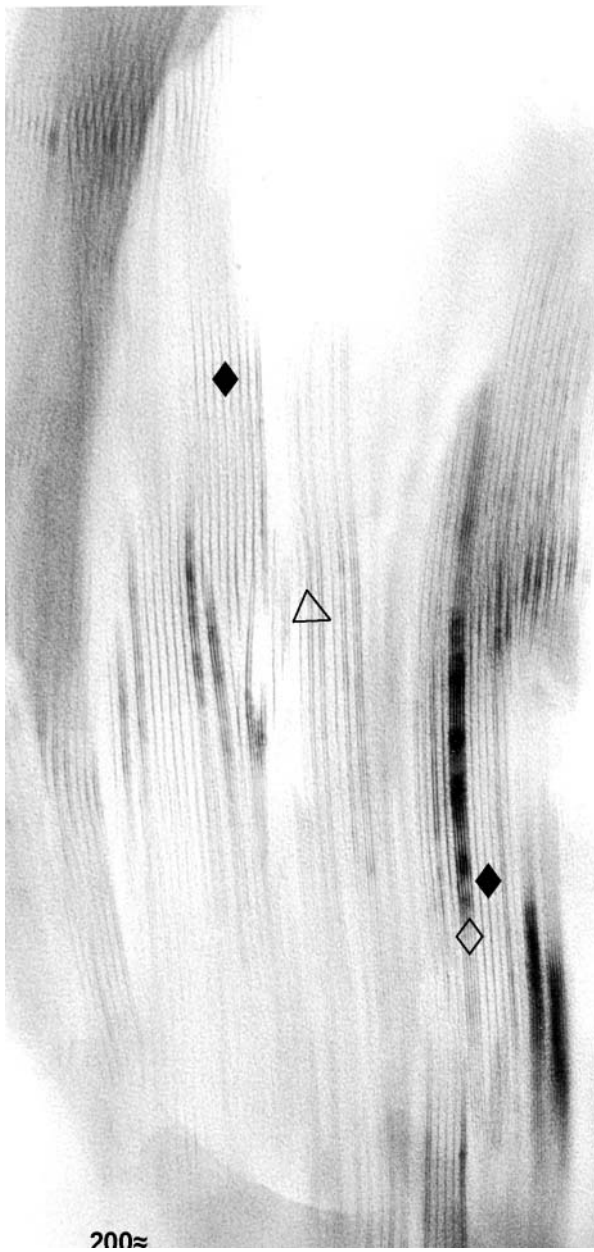

FIGURE 16. HRTEM image of the <2 μm size fraction from the Cap-des-Rosiers Group, McGerrigle Mountains anchizone (sample TM39) after treatment with n_C = 18 showing packets of expandable illite interlayers (solid diamond) occurring together with thin packets of three to five non-expandable 2:1 layers of illite (open diamond) and sequence of double layers with expandable interfaces (open triangle). The co-existence of these phases in the coarse fractions may indicate that illite evolution is a gradual conversion rather than a sharp-step process.

Similarly, chlorites in the <2 μm fractions of the material studied form very thick domains of non-expandable 2:1 layers of 14 Å spacing (Fig. 14). Like illitic material, the chlorite mixed-layers exist mainly in the coarse fractions, with one main difference: the types of mixed-layering in chlorite are limited, i.e., only corrensite-like R1-ordered structures have been described, in contrast to expandable components in illitic materials, which occur in various structures, e.g., in R1-, R3-ordered structures, and expandable illite. This difference may indicate that the prograde modifications of chlorite leads to discrete flakes of chlorite, which thus resembles the evolution of illite but with fewer intermediate steps.

Expandability and peak asymmetry

The first-order basal reflection of illite or white mica from diagenetic and low-grade metamorphic rocks tends to be asymmetrical (Wang et al. 1995). With increasing sharpness of the 10 Å reflection, the asymmetry of the peak decreases. This decrease results from increasing crystallite size with increasing grade. However, as Stern et al. (1991) noticed, a marked change in the asymmetry of 10 Å peak of illite (in addition to the progressively improving IC) in a progressive diagenetic-metamorphic recrystallization sequence also indicates a continuous decrease in the proportion of the expandable (smectitic?) component. Árkai and Tóth (1983) introduced two different parameters to measure asymmetry of the 10 Å reflection, and were able to separate crystallite size and lattice distortion effects.

Expandability and growth mechanism

In the <2 μm fraction, the presence of larger diffracting domains further narrows the illite and chlorite peaks. The dissolution of expandable phases (rectorite-like, R1-ordered structure with high interlayer charge-density typical of vermiculite, and R3-ordered "Kalkberg" structure) occurs simultaneously with the growth of larger crystals of illite (either expandable illite or non-expandable illite) at the expense of smaller crystallites.

Different methods of deconvolution of XRD patterns assuming various degrees of lattice strain have succeeded in obtaining good fit for illitic materials under VLGM conditions (Shata 2000). As stated above, under epimetamorphic conditions, the contribution of expandable layers to the lattice distortion is very low, if any, and the distortion may be entirely due to stacking faults. The resulting very thick micaceous domains observed in HRTEM images of this study seem to have grown in a metamorphic environment. Shata (2000) studied the crystal-size distribution (CSD; size/mean size vs. frequency/maximum frequency) and showed that both illite and chlorite particles have lognormal distributions skewed toward larger sizes. According to Środoń (1999) and Eberl et al. (1998), lognormal distributions indicate surface-controlled, open-system growth. Środoń et al. (2000) evaluated the size distributions of fundamental particles of illite in I-S mixed layers using the Pt-shadowing technique for the TEM. In that study the nucleation of I was found to have ceased at <20% S in the illitic material. In the S range from 100 to 20%, dissolution of single S layers and nucleation of 20 Å thick layers of illite occurred. In the process, the transition from randomly interstratified I-S to an R1-ordered structure took place. In the range from 20 to 0% S, illite crystals may continue to grow by surface-controlled growth. This latter period of illite formation is characterized by three-dimensional growth.

There is another line of evidence supporting the suggestion that well-crystallized illite (with minimum expandability) consists of newly formed crystals that grew in place under conditions of VLGM and is not of detrital origin. The K-Ar ages of the anchimetamorphic samples are 291 to 299 Ma (Shata 2000), which are not only younger than the age of deposition (~450 to ~545 Ma), but they are also younger than the McGerrigle Mountains intrusion (320–360 Ma; de Römer 1974). This was interpreted as illitic materials having first formed under contact-metamorphic conditions, but then progressively having recrystallized during continuing deep burial after the McGerrigle intrusion (Shata 2000).

Expandability of illite

Vali and Hesse (1990), Vali et al. (1991), and Środoń et al. (1990) highlighted the significance of *n*-alkylammonium-ion intercalation for I-S mixed-layer investigations. However, whereas Vali and Hesse (1990) adapted the method to the study of ultrathin sections with the HRTEM, Środoń et al. (1990) cautioned about possible artifacts resulting from the sample-preparation technique. Ultimate proof that the difference between expandable illite and non-expandable illite is due to charge density and is not an artifact, is difficult to achieve. However, more than 30 years of succesful application of the alkylammonium technique to layer-charge determination in mixed-layer clays, first introduced by Weiss (1963) and Lagaly and Weiss (1969), gives us confidence that the observed different behavior of expandable and non-expandable illite reflects a real difference in charge density.

Perspectives and concluding remarks

Use of the *n*-alkylammonium intercalation method highlights the need to redefine expandability and sheds light on the role of expandability affecting IC in the anchizone and epizone. As demonstrated in this contribution, coupling *n*-alkylammonium treatment with both XRD and HRTEM techniques affords the possibility to identify the presence of expandable components in high-grade diagenetic and VLGM illitic clays and to distinguish various types of illite, which cannot be achieved with XRD of ethylene glycol treated samples. In summary, the results of this study of expandability using *n*-alkylammonium intercalation coupled with HRTEM and XRD allow:

1. The investigation of expandable phases by TEM because *n*-alkylammonium intercalation forms stable compounds that do not collapse under the electron beam in the high vacuum of the HRTEM.
2. The differentation between various types of illite, i.e., "expandable illite" and non-expandable "true mica-like" components using long alkyl chains ($12 \leq n_C \leq 18$), which is not possible with glycolation.
3. Differentiation between expandable illite and high-charge vermiculite in illitic materials using short alkyl chains ($6 \leq n_c \leq 11$), whereas these high-charge components do not respond to glycolation.
4. Detection of small amounts of expandable 2:1 layers, i.e., <1% smectite in I-S mixed layers (Weiss et al. 1971), owing to the large increase in the intensity of basal reflections as a consequence of the formation of alkylammonium-clay complexes.
5. The lack of expandability upon glycolation as measured by XRD should not be taken as de facto evidence for the absence of expandable components, since in the present study, we show that clays that do not respond to EG still expand upon *n*-alkylammonium intercalation.
6. One factor affecting the progressive decrease of the FWHM of the basal illite reflection in prograde diagenetic to VLGM sequences is the continuous decrease in the proportion of smectitic (expandable) components as seen in lattice-fringe images under the HRTEM.
7. On the basis of XRD data, the loss of expandable components (either S or small diffracting domains of illite) seems to be accompanied by the formation of small diffracting domains of smectite-free mica. This change suggests that a portion of the I-S and small illite crystals in diagenetic pelitic rocks recrystallize to form a new mineral phase, which then coarsens thermally to form muscovite involving ongoing recrystallization.
8. In the epizone, (expandable) smectitic phases are no longer present and lattice distortion reflected by peak broadening appears to be solely due to stacking faults.
9. In response to high-grade diagenetic to VLGM conditions, chlorite seems to follow reaction pathways generally similar to those followed by I-S, with different amounts and types of intermediate products. The chlorite mixed-layers basically comprise a corrensite-like, R1-ordered layer structure either with an intermediate or a high-charge vermiculite interface. This material is found mainly in the ultrafine fraction. In contrast, the intermediate products during illite evolution are rectorite-like, R1-ordered layer structure either with an intermediate or high-charge vermiculite interface, and R3-ordered structure found in ultrafine (<0.1 μm) fractions, whereas expandable illite is found mainly in the coarser (<2 μm) fraction.

Acknowledgments

This research was supported by grants from the Natural Sciences and Engineering Research Council (NSERC) of Canada to R.H., and Reinhardt scholarships from McGill University and a research stipend from the EM Centre of McGill University to S.S.. The manuscript benefitted from critical comments of journal reviewers R.J. Merriman and L.N. Warr and help from associate editor W. Trzcienski.

References cited

Ahn, J.H. and Peacor, D.R. (1986) Tansmission electron microscope data for rectorite: Implications for the origin and structure of "fundamental particles." Clays and Clay Minerals, 34, 180–186.

Árkai, P. and Tóth, M. (1983) Illite crystallinity: Combined effects of domain size and lattice distortion. Acta Geologica Hungarica, 26, 341–358.

Árkai, P., Merriman, R.J., Robert, B., Peacor, D.R., and Tóth, M. (1996) Crystallinity, crystallite size and lattice strain of illite-muscovite and chlorite: comparison of XRD and TEM data for diagenetic to epizonal pelites. European Journal of Mineralogy, 8, 1119–1137.

Bailey, S.W., Brindley, G.W., Kodama, H., and Martin, R.T. (1982) Report of the Clay Mineral Society Nomenclature for 1980–1981. Clays and Clay Minerals, 30, 76–78.

Brindley, G.W. (1965) Clay-organic studies X. Complexes of primary amines with montmorillonite and vermiculite. Clay Minerals, 6, 91–96.

Cetin, K. and Huff, W.D. (1995) Layer charge of the expandable component of illite/smectite in K-bentonite as determined by alkylammonium ion exchange. Clays and Clay Minerals, 43, 150–158.

Dalla Torre, M., Livi, K.J.T., Frey, M. (1996) Chlorite textures and compositions from high-pressure/low-temperature metashales and metagraywackes, Franciscan complex, Diablo Range, California, USA. European Journal of Min-

eralogy, 8, 825–846.
de Römer, H.S. (1974) Geology and age of some plutons in north-central Gaspé, Canada. Canadian Journal of Earth Science, 11, 570–582.
Drits, V., Eberl, D.D., and Środoń, J. (1998) XRD measurement of means thickness, thickness distribution and strain for illite and illite/smectite crystallite by the Berated-Warren-Averbach technique. Clays and Clay Minerals, 46, 38–50.
Dunoyer de Segonzac, G. (1970) The transformation of clay minerals during diagenesis and low-grade metamorphism: a review. Sedimentology, 15, 281–346.
Eberl, D.D., Drits, V.A. and Srodoń, J. (1998) Deducing growth mechanisms for minerals from the shapes of crystal size distributions. American Journal of Science, 298, 499–533.
Eberl, D.D., Srodoń, J., Lee, M., Nadeau, P., and Northrop, R. (1987) Sericite from the Silverton caldera, Colorado: Correlation among structure, composition, origin, and particle thickness. American Mineralogist, 72, 914–934.
Hesse, R. and Dalton, E. (1991) Diagenetic and low-grade metamorphic terranes of Gaspé Peninsula related to geologic structure of the Taconian and Acadian orogenic belts, Quebec Appalachians. Journal of Metamorphic Geology, 9, 775–790.
Hunziker, J.C., Frey, M., Clauer, N., Dallmeyer, R.D., Friedrichsen, H., Flehmig, W., and Hochstrasser, K. (1986) The evolution of illite to muscovite: mineralogical and isotopic data from the Glarus Alps, Switzerland. Contributions to Mineralogy and Petrology, 92, 157–180.
Islam, S., Hesse, R., and Changnon, A. (1982) Zonation of diagenesis and low-grade metamorphism in Cambro-Ordovician flysch of the Gaspé Peninsula, Québec Appalachians. Canadian Mineralogist, 20, 155–167.
Jiang, W-T. and Peacor, D.R. (1994) Prograde transitions of corrensite and chlorite in low-grade pelitic rocks from Gaspé Peninsula, Quebec. Clays and Clay Minerals, 42, 497–517.
Kisch, H.J. (1983) Mineralogy and petrology of burial diagenesis and incipient metamorphism in clastic rocks. In G. Larson and G.V. Chilingar, Eds., Diagenesis in Sediments and Sedimentary Rocks, p. 289–493. Developments in Sedimentology, 25B, Elsevier, Amsterdam.
——— (1990) Calibration of anchizone: a critical comparison of illite 'crystallinity' scales used for definition. Journal of Metamorphic Geology, 8, 31–46.
——— (1991) Illite crystallinity: recommendations on sample preparation, X-ray diffraction settings, and interlaboratory samples. Journal of Metamorphic Geology, 9, 665–670.
Klug, H.P. and Alexander, L.E. (1974) X-ray diffraction procedures for polycrystalline and amorphous materials, 2nd ed. Wiley, New York.
Krekeler, M.P.S. and Huff, W.D. (1993) Occurrence of corrensite and ordered (R3) illite/smectite (I-S) in a VLGM Middle Ordovician K-bentonite from the Hamburg Klippe, central Pennsylvania. 28th Annual Meeting Abstracts with Programs, Northeastern Section, 25(2), p. 30. Geological Society of America, Boulder, CO.
Lagaly, G. (1979) The "layer charge" of regular interstratified 2:1 clay minerals. Clays Clay Minerals, 27, 1–10.
———(1987) Clay-organic interactions: problems and recent results. Proceedings of International Clay Conference (Tokyo) 1, 61–80.
——— (1994) Layer charge determination by alkylammonium ions. In A.R. Mermut, Ed., Layer Charge Characteristics of 2:1 Silicate Clay Minerals, Clay Mineral Society Workshop Lectures, 6, 1–14. Clay Mineral Society, Boulder, CO.
Lagaly, G. and Weiss, A. (1969) Determination of the layer charge in mica-type layer silicates. In H. Heller, Ed., Proceedings of International Clay Conference, Tokyo, p. 61–80. Israel University Press, Jerusalem.
Laird, D.A., Scott, A.D., and Fenton, T.E. (1987) Interpretation of alkylammonium characterization of soil clays. Soil Science Society American Journal, 51, 1659–1663.
Merriman, R.J. and Peacor, D.R. (1999) Very low-grade metapelites: mineralogy, microfabrics and measuring reaction progress, p. 10–60. In M. Frey and D. Robinson, Eds., Low grade metamorphism, 313 p. Blackwell, Oxford, U.K.
Merriman, R.J., Robert, B., and Peacor, D.R. (1990) A transmission electron microscope study of white mica crystallite size distribution in a mudstone to slate transitional sequence, North Wales, U.K. Contributions to Mineralogy and Petrology, 106, 27–40.
Moore, D.M. and Reynolds R.C. Jr. (1997) X-ray diffraction and the identification and analysis of clay minerals, 2nd ed., 378 p. Oxford University Press, U.K.
Olis, A.C., Malla, P.B., and Douglas, L.A. (1990) The rapid estimation of the layer charges of 2:1 expanding clays from a single alkylammonium ion expansion. Clay Minerals, 25, 39–50.
Ransom, B. and Helgeson, H.C. (1989) On the correlation of expandability with mineralogy and layering in mixed-layer clays. Clays and Clay Minerals. 37,189–191.
Rühlicke, G. and Kohler, E.E. (1981) Note: A simplified procedure for determining layer charge by the n-alkylammonium method. Clay Minerals, 16, 305–307.
Sears, S.K., Hesse, R., and Vali, H. (1998) Significance of n-alkylammonium cation-exchange for the study of 2:1 clay mineral diagenesis, Mackenzie Delta–Beaufort Sea region, Arctic Canada. Canadian Mineralogist 36(6), 1485–1506.
Shata, S. (2000) Illitization and chloritization of illite/smectite and chlorite/smectite mixed-layer clays in high-grade diagenetic and very low-grade metamorphic environments of Gaspé Peninsula, Québec Appalachians, Canada: Problems and solutions, 180 p. Ph.D. Dissertation, McGill University, Montreal, Canada.
Shata, S. and Hesse, R. (1998) Refined XRD method for the determination of chlorite composition and application to the McGerrigle Mountains anchizone n the Quebec Appalachians. Canadian Mineralogist, 36, 1525–1546.
Shau, Y-H, Peacor, D.R., and Essene, E.J. (1990) Corrensite and mixed-layer chlorite/corrensite in metabasalts from northern Taiwan: TEM/AEM, EMPA, XRD, and optical studies. Contribution to Mineralogy and Petrology, 105, 123–142.
Skidmore, W.B. and McGerrigle, H.W. (1967) Geological map of the Gaspé peninsula. Quebec Dept. Natural Resources, Map 1642.
Spurr, A.R. (1969) A low viscosity epoxy resin embedding medium for electron microscopy. Journal of Ultrastructure Research, 26, 31–43.
Środoń, J. (1981) X-ray diffraction of randomly interstratified illite-smectite in mixtures with discrete illite. Clay Minerals,16, 297–304.
——— (1984) X-ray diffraction of illitic materials. Clays Clay Minerals, 32, 337–349.
——— (1999) Nature of mixed-layer clays and mechanisms of their formation and alteration. Annual Reviews of Earth and Planetary Sciences, 27, 19–53.
Środoń, J. and Eberl, D.D. (1984) Illite. In S.W. Bailey, Ed., Mica, 13, p. 495–544. Reviews in Mineralogy, Mineralogical Society of America, Washington, D.C.
Srodoń, J., Anderoli, C., Elsass, F., and Robert, M. (1990) Direct HRTEM measurement of expandability of mixed-layer illite/smectite in bentonite rock. Clays and Clay Minerals, 38, 373–379.
Środoń, J., Eberl, D.D., and Drits, V.A. (2000) Evolution of fundamental -particle size during illitization of smectite and implications for reaction mechanism. Clays and Clay Minerals, 48, 446–458.
St. Julien, P. and Hubert, C. (1975) Evolution of the Taconian Orogen in the Quebec Appalachians. American Journal of Science, 275A, 337–362.
Stern, W.B., Mullis, J., Rehan, M., and Frey, M. (1991) Deconvolution of the first «illite» basal reflection. Schweizerische Mineralogische und Petrographische Mitteilungen, 71, 453–462.
Vali, H. and Hesse, R. (1990) Alkylammonium ion treatment ion treatment of clay minerals in ultrathin section: A new method for HRTEM examination of expandable layers. American Mineralogist, 75, 1443–1446.
———(1992) Identification of vermiculite by transmission electron microscopy and X-ray diffraction. Clay Minerals, 27, 185–192.
Vali, H. and Köster, H.M. (1986) Expanding behavior, structural disorder, regular and random irregular interstratification of 2:1 layer silicates studied by high-resolution images of transmission electron microscopy. Clay Minerals, 21, 827–859.
Vali, H., Hesse, R., and Kohler, E.E. (1991) Combined freeze-etched replicas and HRTEM images as tools to study fundamental particles and multi-phase nature of 2:1 layer silicates. American Mineralogist, 76, 1973–1984.
Vali, H., Hesse, R. and Kodama, H. (1992) Arrangement of alkylammonium ions in phlogopite and vermiculite: An XRD and TEM-study. Clays and Clay Minerals, 40, 240–245.
Vali, H., Hesse, R., and Martin, R.F. (1994) A TEM-based definition of 2:1 layer silicates and their interstratified constituents. American Mineralogist, 79, 644–653.
Wang, H., Stern, W.B., and Frey, M. (1995) Deconvolution of the 10 Å complex: a case study of Helvetic sediments from eastern Switzerland. Schweizerische Mineralogische und Petrographische Mitteilungen, 75, 187–199.
Warr, L.N. and Nieto, F. (1998) Crystallite thickness and defect density of phyllosilicates in low-temperature metamorphic pelites: a TEM and XRD study of clay mineral crystallinity-index standards. Canadian Mineralogist, 36, 1393–1413.
Warr, L.N., and Rice, A.H.N. (1994) Interlaboratory standardization and calibration of clay mineral crystallinity and crystallite size data. Journal of metamorphic Geology, 12, 141–152.
Weiss, A. (1963) Mica-type layer silicates with alkylammonium ions. Clays and Clay Minerals, 10, 191–224.
Weiss, A., Lagaly, G., and Beneke, K. (1971) Steigerung der Nachweisempfindlichkeit von quellungsfähigen Dreischichttonmineralen in Gemengen. Zeitschrift für Pflanzenernährung und Bodenkunde, 129, 193–202.
Wilcoxon, B.R., Ferrell, R.E. Sassen, R., and Wade, W.J. (1990) Illite polytype distribution as an inorganic indicator of thermal maturity in theSmackover Formation of the Manila Embayment, southwest Alabama. Organic Geochemisty, 15, 1–8.
Wybrecht, E., Duplay, J, Piqué, A., and Weber, F. (1985) Mineralogical and chemical evolution of white micas and chlorites, from diagenesis to low-grade metamorphism: data from various size fractions of graywackes (Middle Cambrian, Morocco). Mineralogical Magazine, 49, 401–411.
Yang, C. and Hesse, R. (1991) Clay minerals as indicators of diagenetic and anchimetamorphic grade in an overthrust belt, external domain of southern Canadian Appalachians. Clay Minerals, 26, 211–231.

MANUSCRIPT RECEIVED JANUARY, 30, 2001
MANUSCRIPT ACCEPTED DECEMBER, 31, 2003
MANUSCRIPT HANDLED BY WALTER E. TRZCIENSKI JR.

APPENDIX: CONFIGURATIONS OF *N*-ALKYLAMMONIUM–CLAY COMPLEXES

The exchange of interlayer cations in 2:1 layer silicates with *n*-alkylammonium cation is a method that allows layer charge and charge distribution of expandable 2:1 layer silicates (smectite, vermiculite minerals, and illitic materials) to be determined (Weiss 1963; Brindley 1965; Lagaly and Weiss 1969; Olis et al. 1990; Cetin and Huff 1995). The stoichiometric *n*-alkylammonium cation exchange reaction is a function of alkyl chain-length and the density of the clay interlayer charge:

$$Ca[\text{smectite}] + 2R\text{-}NH_3^+ \leftrightarrow (NH_3)_2[\text{smectite}] + Ca^{2+}$$

with $R\text{-}NH_3^+ = C_nH_{2n+1}NH_3^+$ and n = 6, 7, 8,….18.

The alkylammonium ions in the interlayer space of the 2:1 layer silicate may be oriented in a *trans* configuration, i.e., the zigzag of the chains with a constant cross-sectional area oriented normal to (001) either as a monolayer (13.7 Å), bilayer (17.7 Å), pseudotrimolecular layer (21.7 Å), or a paraffin-type arrangment (Fig. A1), depending on the magnitude of the layer charge (flat-lying for smectite and low-charge vermiculites, and tilting for high-charge vermiculite and expandable illite).

Which one of these different accommodations will be achieved depends on the A_c/A_e ratio. A_c is the area occupied by the flat-lying *n*-alkyl ammonium ions, with n_C being the number of carbon atoms in the alkylchain:

$$A_c = 1.26(4.5)n_C + 14\ (Å^2)$$

where 1.26 is the carbon-carbon bond length in Å, 4.5 is the diameter of the *n*-alkylammonium ion in Å, and 14 is the area occupied by the NH_4^+ group of the alkylammonium ion.

A_e, the equivalent area, is the area that is available for flat-lying monovalent cations in the interlayer space: $A_e = ab/2\xi$, where x is the cation density per half unit cell, and *a*, *b* are unit-cell dimensions of 2:1 layer-silicates per $[2(Si, Al)_4(OH)_{10}]$.

Therefore, $-A_e = 23.5/\xi$ for dioctahedral minerals, and $24.5/\xi$ for trioctahedral minerals).

For short chains, for which $A_e > A_c$, the alkylammonium ions form monolayers. With longer alkyl chains, A_c becomes greater than A_e, and alkylammonium ions rearrange in bilayers. During this transition from monolayer to bilayer, A_c becomes equal to A_e, and

$$\xi = (23.3/5.67^* n_C + 14).$$

The transition to pseudotrimolecular layers occurs where $A_c/A_e \geq 2$. The paraffin-type structure develops with longer chain-lengths where $A_c/A_e > 2$. In other words, with long-chain alkylammonium derivatives of high-charged minerals, in which A_c is largely due to the long chains and A_e is small because of high ξ, the tilt angle α is controlled by the layer charge density. The tilt angle increases to a maximum of 90° for a layer charge of 1.0 per half the unit cell. The tilt angle is calculated from the mean increase in the *d*-values from one to the next higher (and/or longer) alkylammonium chain: $\alpha = \sin^{-1}\delta d / 1.26$.

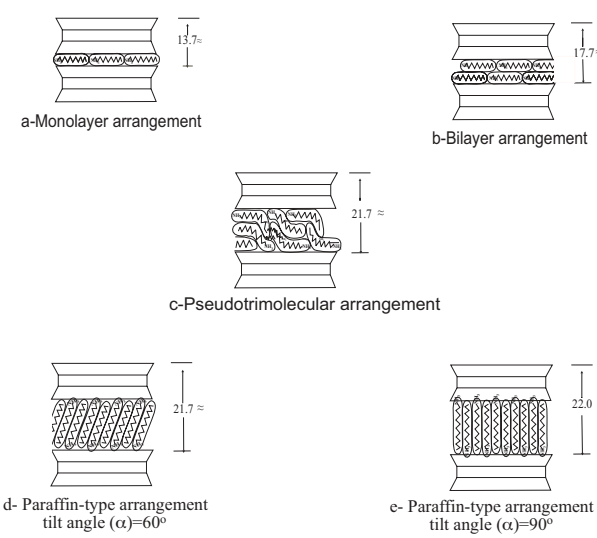

APPENDIX FIGURE 1. Configuration of alkylammonium ions in the interlayer space of different 2:1-layer silicates.